

Roy–Steiner equations for pion–nucleon scattering and the pion–nucleon σ -term

Martin Hoferichter*[†]

Institute for Nuclear Theory, University of Washington, Seattle, WA 98195-1550, USA

E-mail: mhofer@uw.edu

Jacobo Ruiz de Elvira

Albert Einstein Center for Fundamental Physics, Institute for Theoretical Physics, University of Bern, Sidlerstrasse 5, CH–3012 Bern, Switzerland

E-mail: elvira@itp.unibe.ch

Bastian Kubis

Helmholtz-Institut für Strahlen- und Kernphysik (Theorie) and Bethe Center for Theoretical Physics, Universität Bonn, D–53115 Bonn, Germany

E-mail: kubis@hiskp.uni-bonn.de

Ulf-G. Meißner

*Helmholtz-Institut für Strahlen- und Kernphysik (Theorie) and Bethe Center for Theoretical Physics, Universität Bonn, D–53115 Bonn
Institut für Kernphysik, Institute for Advanced Simulation, and Jülich Center for Hadron Physics, Forschungszentrum Jülich, D–52425 Jülich, Germany*

E-mail: meissner@hiskp.uni-bonn.de

We review the determination of the low-energy pion–nucleon scattering amplitude using Roy–Steiner equations. In particular, we focus on the phenomenological determination of the pion–nucleon σ -term, derived in combination with modern precision data on pionic atoms, and address some of the most frequently asked questions regarding our analysis. Finally, we discuss recent applications to nucleon form factors and the determination of low-energy constants in chiral perturbation theory.

*The 9th International Workshop on Chiral Dynamics
17–21 September 2018
Durham, NC, USA*

*Speaker.

[†]These proceedings draw from previous conference contributions [1–4].

1. Introduction

The pion–nucleon (πN) σ -term $\sigma_{\pi N}$ determines the scalar couplings of the nucleon to u - and d -quarks and thus represents a key matrix element required in the search for physics beyond the Standard Model (BSM). This concerns most notably the interpretation of direct-detection searches for dark matter [5–7], but also other search channels in which a scalar current can couple to the nucleon [8–10]. Often, matrix elements that involve currents for which no Standard Model probe exists can only be accessed in lattice QCD, but the σ -term constitutes a notable exception. It is related to πN scattering by means of the Cheng–Dashen low-energy theorem (LET) [11, 12], which connects the scalar form factor of the nucleon to the Born-term-subtracted isoscalar πN scattering amplitude analytically continued into the unphysical region. The corresponding phenomenological determination of the σ -term thus presents a unique opportunity to confront lattice QCD calculations with experiment. The σ -term is also a classic example of chiral dynamics at work. On the one hand, its smallness is a consequence of the vanishing of the leading chiral order, on the other, strong $\pi\pi$ rescattering makes a resummation in dispersion theory mandatory. Accordingly, the scalar channel as such is particularly interesting for BSM applications, see [13–20] for the consequences of chiral symmetry in the dark matter context.

A precision determination of the low-energy scattering amplitude has further applications that extend beyond πN . The response of the nucleon to external currents can be analyzed via a t -channel dispersion relation, and depending on the quantum numbers $\pi\pi$ intermediate states frequently dominate the integral. In particular, for the P -waves, the $\pi\pi$ continuum gives the bulk of the isovector spectral functions of the nucleon electromagnetic form factors, an essential input for the analysis of the proton radius puzzle from electron scattering experiments. Second, the low-energy constants (LECs) that define the chiral expansion of the πN amplitudes also govern the long-range part of the nucleon–nucleon (NN) potential and the three-nucleon force, and thus provide crucial input for a systematic approach to nuclear forces.

2. Roy–Steiner-equation analysis of pion–nucleon scattering

The Cheng–Dashen LET [11, 12] relates the Born-term-subtracted isoscalar amplitude evaluated at the Cheng–Dashen point ($\nu = 0, t = 2M_\pi^2$) to the scalar form factor of the nucleon, evaluated at momentum transfer $t = 2M_\pi^2$. In practice, this LET is often rewritten as

$$\sigma_{\pi N} = \sigma(0) = \Sigma_d + \Delta_D - \Delta_\sigma - \Delta_R, \quad (2.1)$$

where Δ_R represents higher-order corrections in the chiral expansion, which are expected to be small given that chiral logarithms cancel at 1-loop order [21]. Δ_σ measures the curvature in the scalar form factor, Δ_D parameterizes contributions to the πN amplitude beyond the first two terms in the subthreshold expansion, and $\Sigma_d = F_\pi^2(d_{00}^+ + 2M_\pi^2 d_{01}^+)$. As shown in [22], although these corrections are large individually due to strong rescattering in the isospin-0 $\pi\pi$ S -wave, they cancel to a large extent in the difference. For the numerical analysis we use $\Delta_D - \Delta_\sigma = -1.8(2)\text{MeV}$ [23].

In this way, the remaining information on the scattering amplitude is encoded in the subthreshold parameters d_{00}^+ and d_{01}^+ , and these are determined from the solution of Roy–Steiner (RS)

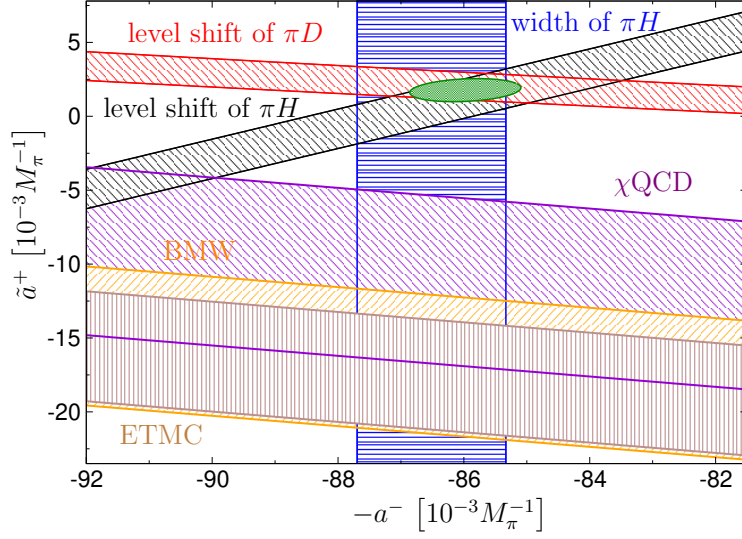


Figure 1: Constraints on the isoscalar and isovector scattering lengths \tilde{a}^+ and a^- from the level shift in pionic hydrogen (black) and pionic deuterium (red) as well as the width of pionic hydrogen (blue). The pionic-atom overlap region (green) lies significantly above the bands from lattice QCD, reinterpreting the σ -term results as a constraint on the scattering lengths. Figure taken from [46].

equations [24]. The complete system includes both the $\pi N \rightarrow \pi N$ (s -channel) and $\pi\pi \rightarrow \bar{N}N$ (t -channel) partial waves, with the physical regions connected via hyperbolic dispersion relations, see [23, 25] for its derivation and [26] for the solution. Therefore, while the basic idea, the combination of analyticity, unitarity, and crossing symmetry in a partial-wave framework, is identical to $\pi\pi$ Roy equations [27–30], the presence of the crossed channel makes the process more closely related to dispersive analyses of πK scattering [31] or $\gamma\gamma \rightarrow \pi\pi$ [32]. In practice, the solution of the πN RS equations is greatly stabilized when the S -wave scattering lengths, known precisely from pionic atoms [26, 33, 34], are imposed as constraints. Final results for the πN partial waves and subthreshold parameters are given in [26], in a form linearized around the pionic-atom input we obtain [35]

$$\Sigma_d = 57.9(9) \text{ MeV} + \sum_{I_s} c_{I_s} \Delta a_{0+}^{I_s}, \quad c_{1/2} = 0.242 \text{ MeV}, \quad c_{3/2} = 0.874 \text{ MeV}, \quad (2.2)$$

where $\Delta a_{0+}^{I_s}$ gives the deviation from the scattering lengths extracted from pionic atoms in units of $10^{-3} M_\pi^{-1}$. The result for the σ -term itself becomes

$$\sigma_{\pi N} = 59.1(2.0)_{\text{CD}}(2.2)_{\text{IB}}(1.6)_{\text{SL}}(0.9)_{\text{RS}} = 59.1(3.5) \text{ MeV}, \quad (2.3)$$

where the various sources of error refer to the Cheng–Dashen remainder, isospin-breaking corrections in the LET [35] (see also [36–38]), the uncertainty in the scattering lengths, and the systematics of the solution of the RS system.

Our central result (2.3) crucially depends on the πN scattering lengths as extracted from pionic-atom spectroscopy measurements [39–41]. Unfortunately, there is persistent tension with recent results in lattice QCD [42–45], which favor a significantly lower value of $\sigma_{\pi N}$ and can indeed

be reinterpreted as another constraint in the scattering-length plane that is inconsistent with the pionic-atom measurements [46], see Fig. 1. Given the role of $\sigma_{\pi N}$ as a benchmark for BSM matrix elements, this discrepancy between lattice QCD and phenomenology urgently needs to be resolved.

3. Frequently asked questions

3.1 Why does your number differ from Gasser, Leutwyler, Sainio?

Our result (2.3) lies significantly above the canonical value $\sigma_{\pi N} \sim 45 \text{ MeV}$ from [47]. This shift can be fully explained just from the input used in the solution of the RS equations, given that the analysis of [47] is based on the scattering lengths and πN coupling constant from the KH80 partial-wave analysis (PWA) [48]. We checked that given this input the KH80 solution is indeed self-consistent [26] and accordingly reproduce the lower σ -term. However, we stress that this input is inconsistent with the modern pionic-atom experiments, most notably in the $I_s = 3/2$ scattering length: $a_{0+}^{3/2}|_{\text{KH80}} = -101(4) \times 10^{-3} M_\pi^{-1}$ vs. $a_{0+}^{3/2}|_{\text{pionic atoms}} = -86.3(1.8) \times 10^{-3} M_\pi^{-1}$, which by means of (2.2) implies a difference of 13 MeV in the σ -term. We also checked that our amplitudes fulfill the forward dispersion relations employed in [47].

3.2 Could it be isospin-breaking corrections?

We believe that this is highly unlikely. The isospin-breaking corrections to the LET analogous to the known large effects in the isoscalar scattering lengths [36,37] are included, and so are isospin-breaking corrections in the pion–deuteron system [33, 34]. Isospin amplitudes are consistently defined in terms of the $\pi^\pm p$ channels, with the corresponding corrections applied to the scattering lengths and the LET to match this definition [26]. In the end, the uncertainty of 2 MeV in (2.3) related to isospin breaking is dominated by a generous estimate for a LEC. It is difficult to see how to generate higher-order effects that could exceed that estimate [46]. In the end, isospin breaking in the LET actually increases $\sigma_{\pi N}$ by 3.0 MeV.

3.3 Why not use chiral perturbation theory to extract the σ -term?

First of all, a chiral analysis of $\sigma_{\pi N}$ requires input for the LECs, typically obtained by a fit to πN phase shifts. Accordingly, the results for $\sigma_{\pi N}$, see e.g. [49, 50], reflect the input chosen for the PWA, with fits to KH80 leading to a lower and those to more modern PWAs [51, 52] to a higher σ -term. More importantly, the one-loop representation proves not sufficiently rigorous for a reliable σ -term extraction: the LET is only fulfilled perturbatively, with relations known to fail for Δ_D and Δ_σ separately; the effect from t -channel D -waves, which is essential in the dispersive analysis, is not captured at one-loop order; relating the subthreshold and the physical region with a chiral representation is problematic, see Sect. 4.2 below; and a simple fit to a PWA neglects isospin-breaking corrections.

3.4 What if the pionic-atom measurements are wrong?

We believe this is unlikely, given that three independent experimental constraints [39–41] and their theoretical interpretation [33, 34, 53–55] produce an overlapping region for two scattering lengths, but further confirmation is of course highly welcome. An independent constraint can be

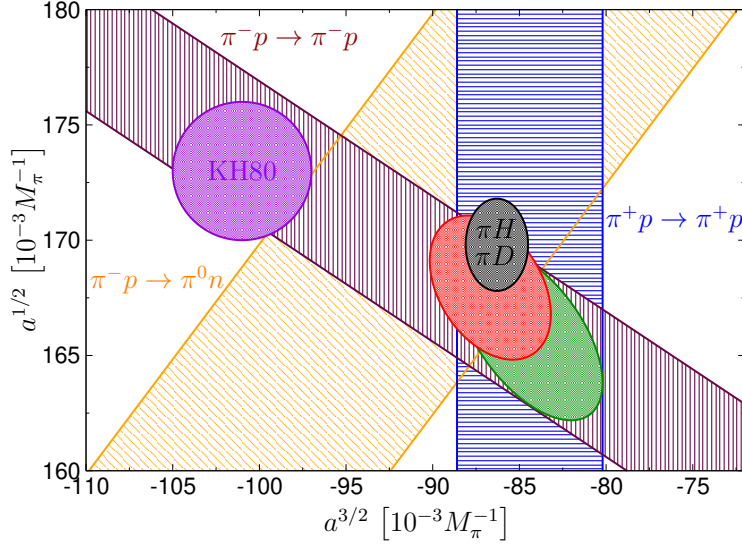


Figure 2: Constraints on the $I_s = 1/2, 3/2$ scattering lengths $a^{1/2}$ and $a^{3/2}$ from $\pi^+ p \rightarrow \pi^+ p$ (blue), $\pi^- p \rightarrow \pi^- p$ (maroon), and $\pi^- p \rightarrow \pi^0 n$ (orange). The combination of the elastic (all) channels leads to the green (red) ellipse. The KH80 and pionic-atom scattering lengths are marked in violet and black, respectively. Figure taken from [56].

obtained by fitting a RS representation to low-energy cross sections data [56], which allows for an alternative albeit slightly less precise determination of the πN scattering lengths. Challenges in this fit include the treatment of the substantial normalization uncertainties in the data base, which implies that existing compilations cannot be used due to a bias to the respective fit model, as well as isospin-breaking corrections. We considered each charge channel separately, with the corresponding scattering length as a free parameter, kept the uncontentious Coulomb piece of the electromagnetic corrections from [57] while treating the rest as an error estimate, and admitted all normalizations as additional fit parameters (to avoid D’Agostini bias [58] setting up an iterative fit strategy [59]). The final results for the scattering lengths are shown in Fig. 2: while the $\pi^- p \rightarrow \pi^- p$ channel is consistent with both KH80 and pionic atoms and the charge-exchange reaction $\pi^- p \rightarrow \pi^0 n$ remains largely inconclusive, the $\pi^+ p \rightarrow \pi^+ p$ data unambiguously decide in favor of pionic atoms. Combining all three channels, we find from the fit to the low-energy cross sections

$$\sigma_{\pi N} = 58(5) \text{ MeV}, \quad (3.1)$$

in perfect agreement with (2.3).

As a by-product we obtain the scattering lengths for the three channels separately, which allows for the first time for a quantification of isospin breaking directly from the data. We find

$$R = 2 \frac{a_{\pi^+ p \rightarrow \pi^+ p} - a_{\pi^- p \rightarrow \pi^- p} - \sqrt{2} a_{\pi^- p \rightarrow \pi^0 n}}{a_{\pi^+ p \rightarrow \pi^+ p} - a_{\pi^- p \rightarrow \pi^- p} + \sqrt{2} a_{\pi^- p \rightarrow \pi^0 n}} = -3.6(4.4)\%, \quad (3.2)$$

in agreement with expectation $R = 0.6(4)\%$ from chiral perturbation theory [37] albeit with significantly larger uncertainties. A more conclusive test would require an improved treatment of electromagnetic corrections.

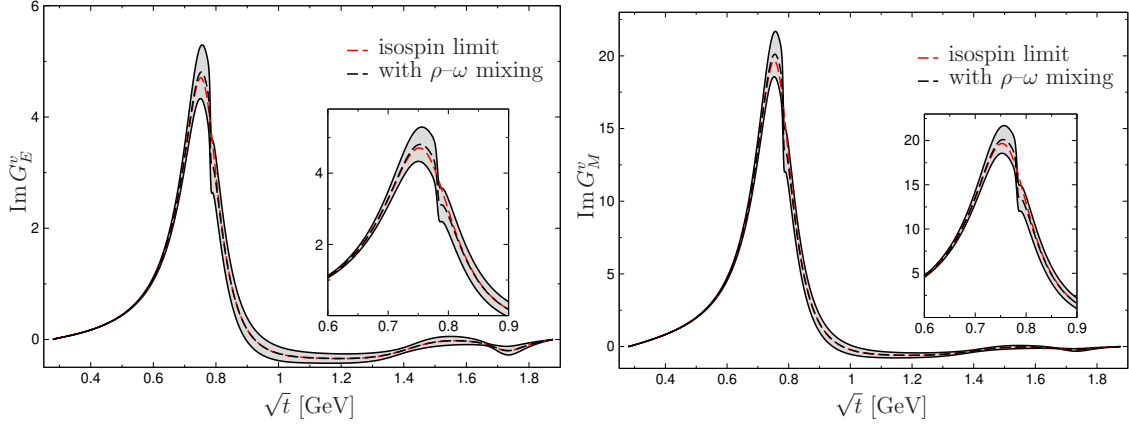


Figure 3: Isovector spectral functions for the electromagnetic form factors of the nucleon. Figure taken from [68].

4. Applications

4.1 Nucleon form factors

The response of the nucleon to external sources is described by form factors, and depending on the quantum numbers their unitarity relation is dominated by $\pi\pi$ intermediate states. The corresponding connection to the partial waves for $\pi\pi \rightarrow \bar{N}N$ has first been pointed out in the context of electromagnetic form factors [60, 61], while the scalar form factor of the nucleon that enters the σ -term correction Δ_σ is arguably the most immediate application for the S -wave [22, 23]. Accordingly, the t -channel P -waves largely determine the isovector spectral functions of the nucleon electromagnetic form factors, which are essential ingredients for analytic form factor parameterizations [62–66]. They also become relevant for the form factors of the antisymmetric tensor current [67].

In [68] we constructed the P -wave spectral functions by combining the RS results for the t -channel partial waves with a dispersive representation for the pion vector form factor (see [69] for a comprehensive analysis of $e^+e^- \rightarrow \pi^+\pi^+$ data in this formalism), including a detailed analysis of isospin-breaking corrections, of which ρ - ω mixing is the most relevant. In particular, these results, available for download at <https://arxiv.org/abs/1609.06722> and reproduced in Fig. 3 for both Sachs form factors, ensure consistency between t -channel partial waves, the pion form factor, and $\pi\pi$ scattering and implement full $\pi\pi$ unitarity, a key advantage of the dispersive representation. Saturating the sum rules for the radii with the $\pi\pi$ spectral functions, we observe remarkably fast convergence, to the extent that together with input for the neutron charge radius [70, 71] we find a slight preference for a small proton radius from the $\pi\pi$ continuum alone.

Recently, it has also been studied to what extent the full dispersive spectral functions can be reconstructed by unitarizing the chiral expansion [72, 73], mainly as a test case for more complicated systems such as hyperon form factors [74] for which the full result is not known. The main conclusions are that Δ -exchange diagrams need to be included and that there is a strong sensitivity to both next-to-leading-order LECs and the chosen unitarization method, so that without imposing the radii to fix parameters the ensuing uncertainties are substantial.

$a_{0+}^- [10^{-3} M_\pi^{-1}]$	heavy-baryon- NN		heavy-baryon- πN		covariant	
	Δ -less	Δ -ful	Δ -less	Δ -ful	Δ -less	Δ -ful
LO	79.4	79.4	79.4	79.4	79.4	79.4
NLO	79.4	79.4(0)	79.4	79.4(0)	80.1	81.9(1)
N ² LO	92.2	92.7(10)	92.9	90.5(9)	89.9	81.7(1.2)
N ³ LO	68.5	96.3(2.0)	58.6	69.1(1.2)	83.8	83.4(1.0)
Pionic atoms			85.4(9)			

Table 1: Convergence pattern of the isovector scattering length a_{0+}^- in two variants of heavy-baryon counting and a covariant formulation, both with and without explicit Δ degrees of freedom. Table taken from [81].

4.2 Low-energy constants

The solution of the RS equations naturally proceeds in terms of subthreshold parameters, which offers a unique opportunity for a systematic determination of πN LECs [75]. In fact, since the subthreshold amplitude can be expanded in a polynomial, at a given chiral order there is a one-to-one correspondence between subthreshold parameters and LECs, so that the LECs can be expressed analytically in terms of the subthreshold parameters. Absent any singularities, one would thus expect the chiral expansion to converge best in the subthreshold region, and, as an added benefit, the subthreshold region is much closer to the kinematics relevant for NN scattering than the physical region for πN . Recent implementations of precision chiral potentials [76, 77] have indeed adopted the accordingly determined LECs.

Surprisingly, though, the chiral convergence of threshold parameters even for the isovector channel is bad if the LECs determined at the subthreshold point are employed. The reason for this behavior could be traced back to loop effects at next-to-next-to-next-to-leading order that are enhanced by $g_A^2(c_3 - c_4) \sim -16 \text{ GeV}^{-1}$, clearly demonstrating that the heavy-baryon amplitude does not converge equally well in the whole low-energy region. The large values of the c_i can be understood from resonance saturation by the $\Delta(1232)$ [78–80], leading to the expectation that the chiral convergence should improve if the Δ is included as an explicit degree of freedom. In [81] we extended the comparison of threshold and subthreshold expansions to the Δ -ful case, both in heavy-baryon counting and a covariant formulation, the results for the isovector scattering length are reproduced in Table 1. One can see that the inclusion of the $\Delta(1232)$ indeed improves the convergence, as expected, but in nearly all cases we also see significant improvements when resumming $1/m_N$ corrections in a covariant set-up. To our knowledge there is currently no convincing explanation as to why the covariant expansion behaves better.

For the application of the LECs to other processes, however, we have now reached the situation where the uncertainties as propagated from the low-energy πN amplitude via the subthreshold parameters are negligible compared to the differences between scheme and chiral order. In [81] we have made these results available for various schemes up to full one-loop order, with and without explicit Δ degrees of freedom.

5. Conclusions

We briefly reviewed RS equations for πN scattering, concentrating on the phenomenological determination of the σ -term by means of the Cheng–Dashen LET. In particular, there are now two completely independent extractions, based on pionic-atom measurements and low-energy cross sections, respectively, that both point to a value close to 60 MeV, making a resolution of the lingering tension with lattice QCD all the more pressing. We also reviewed further applications of the RS solution, to the spectral functions of nucleon form factors and the determination of LECs by matching to chiral perturbation theory in the subthreshold region. In both cases the results are readily available for use elsewhere, for form factor parameterizations that explicitly account for the $\pi\pi$ continuum and in terms of LECs for various schemes and chiral orders including full covariance matrices.

Acknowledgments

Financial support by the DFG (SFB/TR 16, “Subnuclear Structure of Matter,” CRC 110, “Symmetries and the Emergence of Structure in QCD”), the DOE (Grant No. DE-FG02-00ER41132), and the Swiss National Science Foundation is gratefully acknowledged.

References

- [1] B. Kubis, J. Ruiz de Elvira, M. Hoferichter and U.-G. Meißner, PoS CD **15** (2015) 021.
- [2] B. Kubis, M. Hoferichter, J. Ruiz de Elvira and U.-G. Meißner, EPJ Web Conf. **130** (2016) 01006.
- [3] U.-G. Meißner, J. Ruiz de Elvira, M. Hoferichter and B. Kubis, EPJ Web Conf. **137** (2017) 01014.
- [4] J. Ruiz de Elvira, M. Hoferichter, B. Kubis and U.-G. Meißner, PoS Hadron **2017** (2018) 141.
- [5] A. Bottino, F. Donato, N. Fornengo and S. Scopel, Astropart. Phys. **13** (2000) 215.
- [6] J. R. Ellis, K. A. Olive and C. Savage, Phys. Rev. D **77** (2008) 065026.
- [7] A. Crivellin, M. Hoferichter and M. Procura, Phys. Rev. D **89** (2014) 054021.
- [8] V. Cirigliano, R. Kitano, Y. Okada and P. Tuzon, Phys. Rev. D **80** (2009) 013002.
- [9] A. Crivellin, M. Hoferichter and M. Procura, Phys. Rev. D **89** (2014) 093024.
- [10] J. de Vries, E. Mereghetti, C. Y. Seng and A. Walker-Loud, Phys. Lett. B **766** (2017) 254.
- [11] T. P. Cheng and R. F. Dashen, Phys. Rev. Lett. **26** (1971) 594.
- [12] L. S. Brown, W. J. Pardee and R. D. Peccei, Phys. Rev. D **4** (1971) 2801.
- [13] V. Cirigliano, M. L. Graesser and G. Ovanesyan, JHEP **1210** (2012) 025.
- [14] M. Hoferichter, P. Klos and A. Schwenk, Phys. Lett. B **746** (2015) 410.
- [15] M. Hoferichter, P. Klos, J. Menéndez and A. Schwenk, Phys. Rev. D **94** (2016) 063505.
- [16] C. Körber, A. Nogga and J. de Vries, Phys. Rev. C **96** (2017) 035805.
- [17] M. Hoferichter, P. Klos, J. Menéndez and A. Schwenk, Phys. Rev. Lett. **119** (2017) 181803.
- [18] E. Aprile *et al.*, Phys. Rev. Lett. **122** (2019) 071301.

- [19] M. Hoferichter, P. Klos, J. Menéndez and A. Schwenk, Phys. Rev. D **99** (2019) 055031.
- [20] M. Hoferichter, P. Klos, J. Menéndez and A. Schwenk, PoS CD **2018** (2019) 095.
- [21] V. Bernard, N. Kaiser and U.-G. Meißner, Phys. Lett. B **389** (1996) 144.
- [22] J. Gasser, H. Leutwyler and M. E. Sainio, Phys. Lett. B **253** (1991) 260.
- [23] M. Hoferichter, C. Ditsche, B. Kubis and U.-G. Meißner, JHEP **1206** (2012) 063.
- [24] G. E. Hite and F. Steiner, Nuovo Cim. A **18** (1973) 237.
- [25] C. Ditsche, M. Hoferichter, B. Kubis and U.-G. Meißner, JHEP **1206** (2012) 043.
- [26] M. Hoferichter, J. Ruiz de Elvira, B. Kubis and U.-G. Meißner, Phys. Rept. **625** (2016) 1.
- [27] S. M. Roy, Phys. Lett. B **36** (1971) 353.
- [28] B. Ananthanarayan, G. Colangelo, J. Gasser and H. Leutwyler, Phys. Rept. **353** (2001) 207.
- [29] R. García-Martín *et al.*, Phys. Rev. D **83** (2011) 074004.
- [30] I. Caprini, G. Colangelo, and H. Leutwyler, Eur. Phys. J. C **72** (2012) 1860.
- [31] P. Büttiker, S. Descotes-Genon and B. Moussallam, Eur. Phys. J. C **33** (2004) 409.
- [32] M. Hoferichter, D. R. Phillips and C. Schat, Eur. Phys. J. C **71** (2011) 1743.
- [33] V. Baru *et al.*, Phys. Lett. B **694** (2011) 473.
- [34] V. Baru *et al.*, Nucl. Phys. A **872** (2011) 69.
- [35] M. Hoferichter, J. Ruiz de Elvira, B. Kubis and U.-G. Meißner, Phys. Rev. Lett. **115** (2015) 092301.
- [36] J. Gasser *et al.*, Eur. Phys. J. C **26** (2002) 13.
- [37] M. Hoferichter, B. Kubis and U.-G. Meißner, Phys. Lett. B **678** (2009) 65.
- [38] M. Hoferichter, B. Kubis and U.-G. Meißner, Nucl. Phys. A **833** (2010) 18.
- [39] D. Gotta *et al.*, Lect. Notes Phys. **745** (2008) 165.
- [40] T. Strauch *et al.*, Eur. Phys. J. A **47** (2011) 88.
- [41] M. Hennebach *et al.*, Eur. Phys. J. A **50** (2014) 190.
- [42] S. Dürr *et al.*, Phys. Rev. Lett. **116** (2016) 172001.
- [43] Y. B. Yang *et al.*, Phys. Rev. D **94** (2016) 054503.
- [44] A. Abdel-Rehim *et al.*, Phys. Rev. Lett. **116** (2016) 252001.
- [45] G. S. Bali *et al.*, Phys. Rev. D **93** (2016) 094504.
- [46] M. Hoferichter, J. Ruiz de Elvira, B. Kubis and U.-G. Meißner, Phys. Lett. B **760** (2016) 74.
- [47] J. Gasser, H. Leutwyler and M. E. Sainio, Phys. Lett. B **253** (1991) 252.
- [48] R. Koch and E. Pietarinen, Nucl. Phys. A **336** (1980) 331.
- [49] N. Fettes and U.-G. Meißner, Nucl. Phys. A **679** (2001) 629.
- [50] J. M. Alarcón, J. Martin Camalich and J. A. Oller, Phys. Rev. D **85** (2012) 051503.
- [51] M. M. Pavan, I. I. Strakovsky, R. L. Workman and R. A. Arndt, πN Newslett. **16** (2002) 110.
- [52] R. L. Workman *et al.*, Phys. Rev. C **86** (2012) 035202.

- [53] V. Lensky *et al.*, Phys. Lett. B **648** (2007) 46.
- [54] V. Baru *et al.*, Phys. Lett. B **659** (2008) 184.
- [55] V. Baru *et al.*, Eur. Phys. J. A **48** (2012) 69.
- [56] J. Ruiz de Elvira, M. Hoferichter, B. Kubis and U.-G. Meißner, J. Phys. G **45** (2018) 024001.
- [57] B. Tromborg, S. Waldenstrøm and I. Øverbø, Phys. Rev. D **15** (1977) 725.
- [58] G. D’Agostini, Nucl. Instrum. Meth. A **346** (1994) 306.
- [59] R. D. Ball *et al.* [NNPDF Collaboration], JHEP **1005** (2010) 075.
- [60] W. R. Frazer and J. R. Fulco, Phys. Rev. **117** (1960) 1603.
- [61] W. R. Frazer and J. R. Fulco, Phys. Rev. **117** (1960) 1609.
- [62] G. Höhler *et al.*, Nucl. Phys. B **114** (1976) 505.
- [63] P. Mergell, U.-G. Meißner and D. Drechsel, Nucl. Phys. A **596** (1996) 367.
- [64] M. A. Belushkin, H.-W. Hammer and U.-G. Meißner, Phys. Rev. C **75** (2007) 035202.
- [65] R. J. Hill and G. Paz, Phys. Rev. D **82** (2010) 113005.
- [66] I. T. Lorenz, U.-G. Meißner, H.-W. Hammer and Y.-B. Dong, Phys. Rev. D **91** (2015) 014023.
- [67] M. Hoferichter, B. Kubis, J. Ruiz de Elvira and P. Stoffer, Phys. Rev. Lett. **122** (2019) 122001.
- [68] M. Hoferichter *et al.*, Eur. Phys. J. A **52** (2016) 331.
- [69] G. Colangelo, M. Hoferichter and P. Stoffer, JHEP **1902** (2019) 006.
- [70] L. Koester *et al.*, Phys. Rev. C **51** (1995) 3363.
- [71] S. Kopecky *et al.*, Phys. Rev. C **56** (1997) 2229.
- [72] S. Leupold, Eur. Phys. J. A **54** (2018) 1.
- [73] J. M. Alarcón and C. Weiss, Phys. Rev. C **97** (2018) 055203.
- [74] C. Granados, S. Leupold and E. Perotti, Eur. Phys. J. A **53** (2017) 117.
- [75] M. Hoferichter, J. Ruiz de Elvira, B. Kubis and U.-G. Meißner, Phys. Rev. Lett. **115** (2015) 192301.
- [76] D. R. Entem, R. Machleidt and Y. Nosyk, Phys. Rev. C **96** (2017) 024004.
- [77] P. Reinert, H. Krebs and E. Epelbaum, Eur. Phys. J. A **54** (2018) 86.
- [78] V. Bernard, N. Kaiser and U.-G. Meißner, Int. J. Mod. Phys. E **4** (1995) 193.
- [79] V. Bernard, N. Kaiser and U.-G. Meißner, Nucl. Phys. A **615** (1997) 483.
- [80] T. Becher and H. Leutwyler, Eur. Phys. J. C **9** (1999) 643.
- [81] D. Siemens *et al.*, Phys. Lett. B **770** (2017) 27.